が42施設（58.3%）であった。また各月3～6例は11施設，3例以下は7施設であった。

設問2.での使用輸血量の分布については，400～1000mlが34施設，1000～2000mlが32施設，2000～3000mlでは7施設であり，3000ml以上の回答はなかった。すなわち全体の90.4%が400～2000mlの輸血量の範囲であったが，さらにその51.5%は400～1000mlの範囲にあった。

設問3.にあった輸血する決断から実際の輸血開始までの時間は，5分以内が3施設，15分以内が16施設，30分以内では29施設であったが，30分以上とするものも23施設あった。すなわち15分以内とする回答は全体の26.7%で，15分以上が73.2%となっていた。

設問4.の救急部から該当部門への輸血血液供給依頼から実際の使用まで所要時間について，日勤帯と夜勤帯とに差がないと回答したのは37施設であった。夜勤帯で長くなると回答したのは32施設であったが，逆に日勤帯より夜勤帯のほうが迅速に施行できるとの回答が2施設よりあった。

設問5.のinformed consent受領の仕方で，informed consentなしで輸血を施行すると回答した施設が25施設，必ずinformed consentを行って輸血を施行する施設が43施設であった。さらに原則的に患者本人からinformed consentを取ると回答したのは4施設であり，informed consentを家族も含めて取るのは4施設，本人，家族ならびにその他いずれかからとするのは36施設であった。

設問6.の大量輸血での処置および検査項目に関するアンケートでは，膠質液の使用，凝固能の検査，電解質の検査，循環系のモニターを併せて行っているとする施設が15施設，溶血，肝機能，鉄代謝のチェックも含めてすべての検査を行うとする施設が8施設あった。しかし膠質液を使用し，凝固能検査，電解質の検査の3項目を行うとする施設は12施設あり，その他の項目との組み合わせを含めこの3項目は49施設，67.1%で行われていた。

設問7.における輸血後感染症に関する検査は救急部，および他診療科で43施設，63.2%において施行され，患者からの依頼があったときのみ施行する施設は25施設であった。

設問8.の輸血後の不規則抗体の発現に関して，検査しているとする27施設に対して，検査していない施設は44施設（61.9%）であった。

今後臨床に導入されるであろう人工赤血球に関する設問9.で，すでに論文などにて人工赤血球についてなんらかの見識を持っているとの回答は58名（80.5%）であったが，まったく情報を得ていないとする回答14名（19.4%）も認められた。

設問10.に対しては条件しだいでは人工赤血球を使用したいとする回答を含め，使用したいとする回答は20名（25%）であったのに対し，不確定要因を含めて使用しないとする回答が60名（75%）であった。

設問11.の酸素運搬能以外に人工赤血球に必要な条件として循環血液量維持とする回答は60名（78.9%），血液粘度の維持は13名（16.6%）の回答があったが，それ以外に止血機能を妨げない，生体内ラジカルの消去，赤血球同様の変形能，浸透圧の維持，即使用される利便性などがあった。

設問12.での人工赤血球の予想使用量上限に関しては100mlまでとする回答はなく，250mlが3名（4.3%），500mlが20名（28.9%）で，1000ml以上の使用とする回答は46名（66.6%）であった。

もし人工赤血球の臨床使用が可能となっていた場合に緊急輸血に対してどれくらいの頻度で使用される可能性があるかとの設問13.に対して，初期段階では輸液にて対応するので該当症例はないとする回答は5施設（7.1%），毎日使用する症例があるとする回答が4施設，1～6症例／週が27施設，1～6症例/月が34施設であった。すなわち毎月使用する可能性があるとする回答は65施設（92.8%）で，さらに毎週使用する可能性のある施設も31施設（44.2%）あった。

設問14.で赤血球製剤使用に関するinformed consentが受領できるまでの人工赤血球の使用に関しては，informed consent受領と関係なく使用するとの回答が57名（79.1%），晶質液中心にて，あるいはその他の方法にて対応するが15名（20.8%）であった。

病院外での救急救命処置としての設問15.では，呼吸管理のみが6名，呼吸管理と体液管理（晶質液単独，膠質液との併用）が33名，さらにこれらに人工赤血球を併用した管理が33名であり，人工赤血球使用を併用可と回答したのは全体の45.8%に相当していた。

設問16.での人工赤血球の有効半減期に対して，2時間は必要との項目を選択したのは10名，12時間が28名（40.0%），24時間が26名（37.1%），さらに長時間を必要とする回答は6名であった。

設問17.での人工赤血球の網内系への影響については，治療上問題とならないとする回答が29名

(42.0%) であったのに対して，問題となると考えるのは40名 (58.0%) であった。とくに易感染性を懸念する見解が25名 (36%) にみられた。しかし一方，逆に生体からのメディエータの遊離を少なくして反応を緩和する可能性があるとする意見が2名 (3%) に，感染以上に出血死の回避が先決とする意見が3名 (4%) にみられた。

設問18.での人工赤血球への期待には33名から回答が得られたが，膠質・晶質液にはない酸素運搬輸液であること9名 (27.2%)，必要時での即応性について言及した意見8名 (24.2%)，輸血に伴う副作用・合併症の回避を挙げた意見4名 (5.7%) などが主なものであった。

Ⅲ 考　察

アンケートの回収率が39.8%とやや低率であったが，今回の調査で目的とした要点は得られたものと思われた。今回の調査に協力いただいた日本救急医学会評議員の方の多く (80.5%) はすでに人工赤血球に関してなんらかの見識を持っておられた。そしてもし人工赤血球が臨床使用可能となった場合には毎週でも使用する可能性のある施設は31 (44.2%) であることは現在の人工赤血球の有効性 (有効作用時間)，副作用の認容 (網内系への影響) に関する回答率とも一致している。また使用輸血量は400～1000mlとする施設が51.5%となっていたが，このことは最近の日本血液代替物学会が提案した“人工酸素運搬体製造に関する基本的留意事項 (案)”に対して解説した論文[5]で人工赤血球の使用量を一応，20ml/kgと唱えていることとも一致する。すなわち現在開発が進められている人工赤血球で救急患者の半数の輸血に対処できることを示している。一方，人工赤血球使用量への希望は1000ml以上とする回答が全体の66.6%を占めているので，これは今後の人工赤血球開発に対する課題であり，さらなる改良が必要と思われる。

人工赤血球に期待された事項中，もっとも多かったのは確実な酸素運搬能，そして組織への酸素供給であった。またこのような人工赤血球の循環血液内での有効時間については12時間とするものを含め，24時間とする回答が半数を占めているが，現在開発中の人工赤血球の投与後循環血液中滞留半減時間は約30時間[6]と推定されるので，まず多くの現場からの要望に応えられると思われる。しかし人工赤血球内に包埋されているヘモグロビンのメトヘモグロビンへの変化の半減時間に関してはいまだヒトでのデータがなく，ラットでの研究では16～18時間[7,8]となっている。ラットでのデータがそのままヒト，すなわち臨床例には適応されないので，今後の臨床研究で検討しなければならない事項である。

人工赤血球が必要時にただちに使用できることにはとくに大きな期待がある。現行の輸血医療では患者，あるいはその関係者からの輸血施行の informed consent を得るのに時間を要し，さらに輸血発注から実際の輸血までに15分以上の時間を要することが今回の調査で示されている。これに反し現在わが国で開発が進められている人工赤血球は，室温での保存で少なくとも2年間の品質安定性が確認されている[4]。このことは人工赤血球は一般治療薬として用いることができることを示しており，救急部の薬品棚，あるいは救急車の中にも常備することが可能であり，よりよい救命効果が得られると期待される。

さらに人工赤血球への期待には輸血に伴う副作用，合併症を回避したいとの願いが含まれていることも認められた。人工赤血球には血液型がなく，いわゆる universal blood である。したがって血液型の取り違えに伴う輸血事故の発生，あるいは遅発性溶血反応などの免疫性輸血合併症を防止できる。さらに一般輸血に伴う不規則抗体の発生が回避できる。一般輸血でのその発生率は3.1～36.4%[9~11]に及ぶと報告されていて，少なくとも5～10%は生じるのではないかと推測されている。輸血が繰り返される場合での合併症を考えると，この数値は軽視できない。ただ今回の調査では輸血後不規則抗体発生に関する一般的な関心は少ないように思えた。

人工赤血球の製造過程においてはウイルス，細菌などの病原体の不活性化も加えられている。そのため輸血性感染症の回避は確実で，この点に関しても人工赤血球への期待が今回の調査に認められた。

現在開発中の人工赤血球はヒトのヘモグロビンをリポソームの二重膜内に包埋したものであるが，これを生体の循環血液中に投与した際には異物と認識され生体の網内系で捕捉される。したがって投与後一時的に生体の網内系の機能が低下し，その後はむしろ亢進する[7]。この点に関してなんらかの危惧を抱く意見もみられる。しかし生体の抵抗力への危惧よりも出血に伴う生命の危機からの脱出を優先すべきであるとの意見もあり，むしろ蘇生を目的とした人工赤血球としての意義が重要視されるべきではないかと思われる。

現在開発中の人工赤血球，すなわちリポソーム包

埋ヘモグロビンを生理食塩液に浮遊させた製品では膠質浸透圧がなく，投与後の血液量維持効果に欠ける。それゆえに使用量の上限が定められている。日本血液代替物学会が提案した“人工酸素運搬体製造に関する基本的留意事項（案）”に対する解説論文[5]でも20ml/kg以上の量を使用する際にはなんらかの膠質液の併用を推奨している。ヘモグロビン包埋リポソーム粒子を膠質液に浮遊させた製品を作製する考えもあるが，臨床の現場では人工赤血球，すなわちヘモグロビン包埋リポソーム粒子投与量と膠質液投与量との比率は各症例ごとに異なる可能性があり，むしろこのように生理食塩液に浮遊させた人工赤血球と膠質液とは別個に投与することの方が現実的ではないかと思われる。

ま と め

今回，日本救急医学会の評議員を対象として救急医療現場での輸血医療の現状と将来開発される人工赤血球への期待についても調査を行った。その結果，現在，救急部での患者管理上，必要とする輸血用血液の少なくとも50％を開発中の人工赤血球で代替できることが認められた。またさらに投与後の酸素運搬機能維持時間についても半数の施設からの期待を満足させることも認められた。そして人工赤血球が速やかに臨床使用されることへの期待が大きいこと，とくにその保存が容易なこと，universal bloodとして使用できること，副作用・合併症の回避ができることへの期待が認められた。

謝辞：この調査にご協力いただいた日本救急医学会の各評議員の方々に心からの謝意を呈する。またこの調査は厚生労働省科学研究（医薬品・医療機器等レギュラトリーサイエンス総合研究事業）「人工赤血球の安全性向上に関する研究」研究事業の補助研究費の支援により行われた。

【文　献】

1) Sloan EP, Koenigsberg M, Gens D, et al：Diaspirin cross-linked hemoglobin (DCLHb) in the treatment of severe traumatic hemorrhagic shock：A randomized controlled efficacy trial. JAMA 282：1857-1864, 1999.
2) Spahn DR, van Brempt R, Theilmeier G, et al：Perflubron emulsion delays blood transfusions in orthopedic surgery. Anesthesiology 91：1195-1208, 1999.
3) Gawryl MS：Hemopure：Clinical development and experience. 人工血液11：46, 2003.
4) Kobayashi K, Horinouchi H, Watanabe M, et al：Safety and efficacy of hemoglobin-vesicles and albumin-hemes. In：Kobayashi K, Horinouchi H, Tsuchida E, ed. Artificial Oxygen Carrier：Its Front Line. Springer, Tokyo, 2005, pp 1-21.
5) 高折益彦：“人工酸素運搬体作製に関する基本的留意事項”を解説する．人工血液 13：104-111, 2005.
6) Sakai H, Horinouchi H, Masada Y, et al：Metabolism of hemoglobin-vesicles (artificial oxygen carriers) and their influence on organ functions in a rat model. Biomaterials 25：4317-4325, 2004.
7) Tsutsui Y, Kimura T, Ishizuka T, et al：Duration of efficacy NRC (Neo Red Cell) in a rat hemodilution model. 人工血液 10：36-41, 2002.
8) 宗慶太郎, Klipper R, Goins B：ヘモグロビン小胞体の体内動態解析．人工血液 12：53, 2004.
9) Cox JV, Steane E, Cummingham G, et al：Risk of alloimmunization and delays hemolytic transfusion reactions in patients with sickle cell disease. Arch intern Med 148：2485-2489, 1988.
10) Fluit CRMG, Kunst VAJM, Drenthe-Schonk AM：Incidence of red cell antibodies after multiple blood transfusion. Transfusion 30：532-535, 1990.
11) Redman M, Regan F, Contrera M：A prospective study of the incidence of red cell allo-immunisation following transfusion. Vox Sang 71：216-220, 1996.

〔原稿受理日　2006年9月27日・受領No. 2221〕

Microvascular Reviews and Communications

Vol.1 No.1

Sampling rate-dependent RBC velocity in intraparenchymal single capilaries of rat cerebral cortex

Miyuki Unekawa[1], Minoru Tomita[1], Takashi Osada[1], Yutaka Tomita[2], Haruki Toriumi[1] and Norihiro Suzuki[1]

[1] Department of Neurology, School of Medicine, Keio University, Tokyo, Japan

[2] Institute of Brain and Blood Vessels, Mihara Memorial Hospital, Isesaki, Gunma, Japan

Abstract

We previously reported that the average velocity of RBC in single capillaries in anesthetized rat cerebral cortex measured at 250 frame/s was 1.43±1.03 mm/s under physiological conditions. Since we have noticed that the apparent average velocity tends to be higher when the frame (sampling) rate is increased, we investigated in detail the velocity profile at different frame rates. In anesthetized rats, intravenously injected FITC-labeled RBCs were detected in the intraparenchymal tissue through a cranial window at 125, 250 and 500 frames/s with a high-speed laser-scanning confocal fluorescence microscope. RBC velocity and number of RBCs were automatically calculated with Matlab® domain our own software (KEIO-IS2). The RBC velocity in capillaries was found to be dependent upon frame rate, with average values of 0.85±0.43 mm/s at 125 frames/s, 1.34±0.73 mm/s at 250 frames/s and 2.09±1.81 mm/s at 500 frames/s. The velocity distribution was similar among different rats and most values lay within a relatively small range around 1.0 mm/s at any frame rate examined. We conclude that some RBCs, which flow at high speed, are missed at lower frame rates. [MVRC 1(1): 12-15, 2007]

Key Words: frame rate dependent RBC velocity, high-speed confocal fluorescence microscopy, intraparenchymal single capillary

Received; December 25, 2006, Accepted; January 11, 2007

To whom correspondence should be addressed: Dr. Miyuki Unekawa,
Department of Neurology, School of Medicine, Keio University,
35 Shinanomachi, Shinjuku-ku, Tokyo 160-8582, Japan
TEL: +81-3-3353-1211(2316) FAX: +81-3-3353-1272

Introduction

We have reported that the average velocity of red blood cells (RBCs) in single capillaries in anesthetized rat cerebral cortex obtained with a high-speed laser scanning confocal fluorescence microscope at 250 frame/s was 1.43±1.03 mm/s with a range of 0.67 to 3.51 mm/s under physiological conditions[1]. However, we noticed that the average velocity tends to be higher when the sampling rate is increased, so in this study, we systemically examined the sampling rate dependence of the increase in order to obtain the real, or at least a closer-to-real, RBC velocity in intraparenchymal single capillaries.

Material and Methods

Prior to the experiments, fluorescein isothiocyanate (FITC)-labeled RBCs were prepared from freshly drawn rat whole blood as reported by Seylaz et al.[2]. Fifteen Wistar rats anesthetized with urethane were fixed in a head holder. A skull window was opened in the temporo-parietal region and a glass cover slip was placed over it. A femoral artery and a femoral vein were catheterized for blood pressure monitoring and injection of tracers, respectively. After removal of the dura, 0.5 ml of a suspension of labeled RBCs was intravenously injected into the circulating blood. The labeled RBCs appearing in a region of interest (so-called "avascular area rich in capillaries") of the cerebral cortex were recorded with a laser-scanning confocal fluorescence microscope at 125, 250 and 500 frames/s, and the obtained images were analyzed with MATLAB® domain our own software, KEIO-IS2. The program exploits the above-threshold light intensity of bright, round particles (FITC-labeled RBCs) on a dark background to track the particles automatically. The centroid, which was immediately calculated by the computer, was positioned automatically by the MATLAB® software at the geometric center of the connected pixels and the displacement of the centroid in subsequent frames was analyzed. The KEIO-IS2 software built up the tracks of moving RBCs through capillaries frame-by-frame and calculated the velocities of individual RBC in mm/s from the displacement distance divided by the frame interval. The computer conducted the calculations automatically, numbering RBCs in the order of appearance, frame-by-frame for consecutive frames from the specified first frame to the specified last frame.

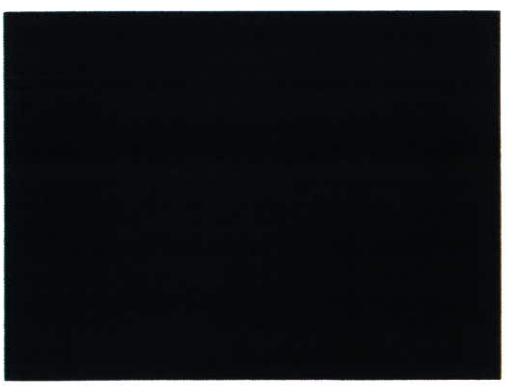

Fig. 1A. An example of "slow video" motion picture which was obtained from original video clip by piecing every 5 frames and stacking together. Therefore, the speed was reduced (see text for explanation).

Results and Discussion

A typical set of results is shown in Fig. 1A, B, C, and D. Fig. 1A is a motion picture whose frames have been chopped every 5 frames from an original 500 frames/s video clip and stacked together. This procedure was done because the original video was too fast to be seen. The moving RBCs in the original video clip were automatically tracked and numbered in different colors for a period of 1 second (Fig. 1B), and the average RBC velocity was calculated automatically for each track by the computer. Figs. 1C and D represent the velocity map and number map of RBCs recognized by the computer. By collocating capillary tracks with those recorded on video tape, the RBC tracks in capillaries were discriminated from those in other vessels (non-capillaris) such as veins. The average velocities of RBCs in capillaries were found to increase with increasing frame rate: 0.85 ± 0.43 mm/s at 125 frames/s (n=5), 1.34 ± 0.73 mm/s ± at 250 frames/s (n=9) and 2.09 ± 1.81 mm/s at 500 frames/s (n=11) (Fig. 2 and Table). The average RBC velocity in non-capillary vessels also increased with increasing frame rate. Velocities both in capillaries and non-capillary vessels tended to be distributed in a similar pattern on velocity range, so that it was impossible to discriminate between types of vessels based on these velocity values alone. The velocity distribution in capillaries was similar among different rats and most

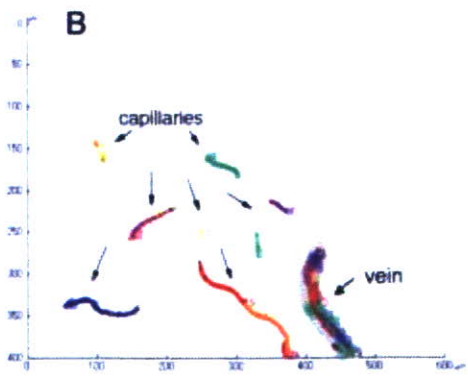

Fig. 1B. To show 2-D RBC tracking map which was obtained from the above original video clip with KEIO-IS2. RBC tracks are shown in different colors automatically numbered in order of appearance. Capillaries were identified with criteria of a diameter less than 10μm. Shadowed tracks are those of non-capillary vessels presumably a vein.

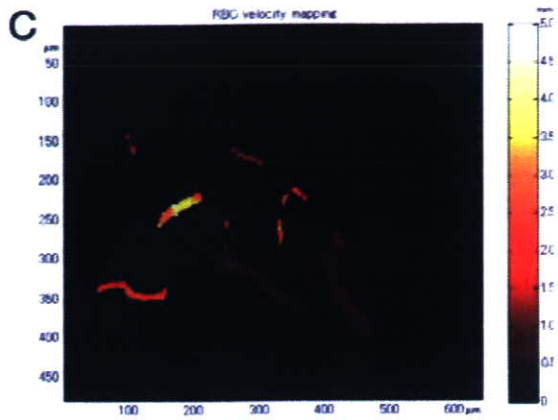

Fig. 1C. RBC velocity map obtained from the same video clip as used above.

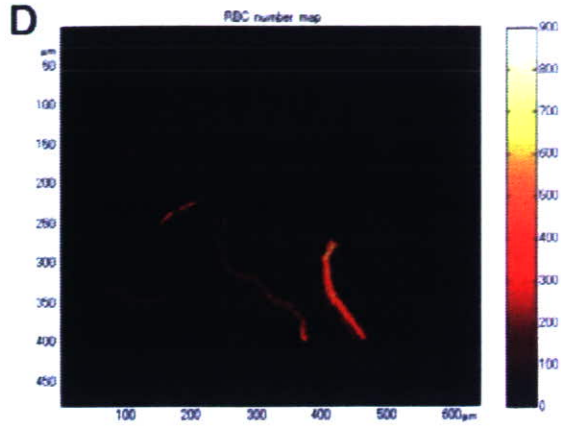

Fig. 1D. RBC number map which was also obtained from the same video clip as used above.

values lay within a relatively small range between 0.5 and 2 mm/s at any frame rate examined (Fig. 3). The frame rate dependency as the higher velocity obtained at higher frame rate was due to RBCs that were uncounted at lower frame rate, because they had moved too fast to be captured, but became detectable at the higher frame rate. Furthermore, both the appearance of RBCs and the calculated velocity in a single capillary fluctuated during 10 sec, but the range of fluctuation was similar at every frame rate examined (Fig. 4A). In another capillary, relatively high velocity was obtained only at higher frame rate (Fig. 4B). This suggests that there are some capillaries in which RBCs move too quickly to be detected at low frame rate. In summary, the average value of RBC velocity in capillaries automatically calculated by computer analysis of high-speed images were found to be higher than those reported in the literatures[3,4], especially when recorded at a higher frame rate. The frame rate dependence arose because some RBCs travelling at high velocity were missed at lower frame rates. It must be cautious that different average RBC velocity values are obtained for the same microvasculature depending on frame rates of the camera. Finally, another question arises that if we can call such a channel with high speed RBCs "capillary" although they have the same diameter as capillaries.

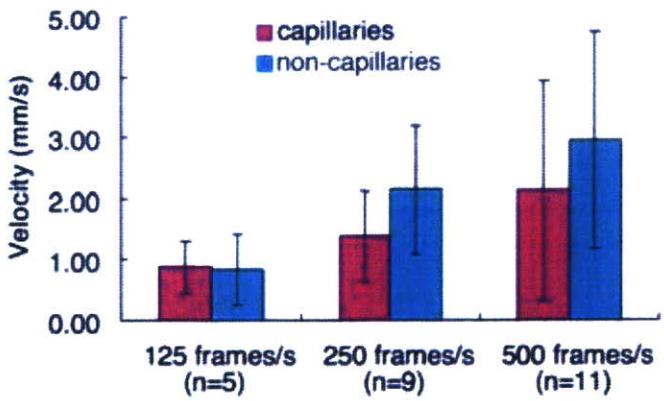

Fig. 2. To show frame rate dependency of average velocities of RBC in capillaries (red column) and non-capillary vessels (blue column) obtained at frame rates of 125, 250 and 500 frames/s.

Frame rate (frames/s)	125	250	500
Number of animals	5	9	11
RBC velocity in capillaries (mm/s)	0.85 ± 0.43	1.34 ± 0.73*	2.09 ± 1.81**
Total number of RBC	163 ± 88	480 ± 183**	710 ± 375**
Number of RBC in capillaries	49 ± 31	93 ± 31*	108 ± 91
% of RBC in capillaries	28.3 ± 16.0	20.7 ± 9.5	16.5 ± 8.1

Table. Average velocity of RBCs in capillaries, total number of detected RBC tracks, number of RBC tracks detected in capillaries, and ratio of RBCs in capillaries to total number of RBCs. * and ** indicate statistically significant differences when compared with the value at 125 frames/s with $p<0.05$ and $p<0.01$, respectively.

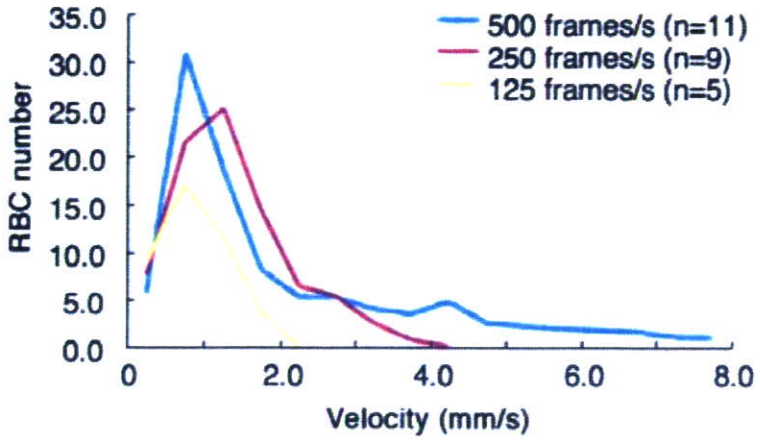

Fig. 3. Variation in velocity distribution. Values are stratified for every 0.5 mm/s. Total appearance of RBC tracks in each range of velocity is divided by the number of rats.

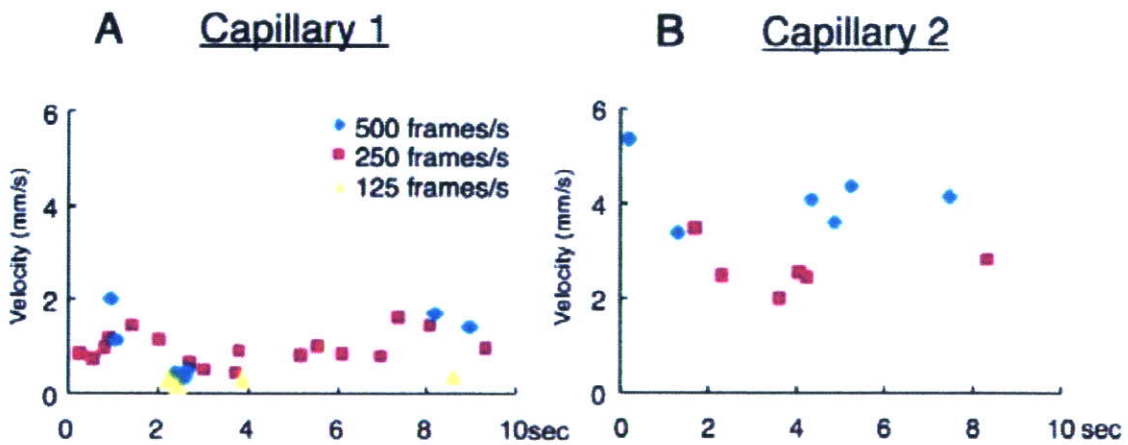

Fig. 4. Fluctuation of RBC velocity in a single capillary (A) and in another capillary (B) in the same rat at different frame rates.

Rerefences

(1) Unekawa M, Tomita M, Osada T, Tomita Y and Suzuki N. RBC velocity in intraparenchymal capillaries of the rat brain and its fluctuation. Microcirc Ann., 21; 85-86; 2005.

(2) Seylaz J, Charbonne R, Nanri K, Von Euw D, Borredon J, Kacem K, Meric P, and Pinard E. Dynamic in vivo measurement of erythrocyte velocity and flow in capillaries and of microvessel diameter in the rat brain by confocal laser microscopy. J Cereb Blood Flow Metab 19: 863-870, 1999.

(3) Hudetz AG. Blood flow in the cerebral capillary network: a review emphasizing observations with intravital microscopy. Microcirculation 4: 233-52, 1997.

(4) Kleinfeld D, Mitra PP, Helmchen F, and Denk W. Fluctuations and stimulus-induced changes in blood flow observed in individual capillaries in layers 2 through 4 of rat neocortex. Proc Natl Acad Sci USA 95: 15741-15746, 1998.

Microcirculation, 15: 163–174, 2008
Copyright © 2008 Informa Healthcare USA, Inc.
ISSN: 1073-9688 print / 1549-8719 online
DOI: 10.1080/10739680701567089

informa
healthcare

Automated Method for Tracking Vast Numbers of FITC-Labeled RBCs in Microvessels of Rat Brain *In Vivo* Using a High-Speed Confocal Microscope System

MINORU TOMITA,* TAKASHI OSADA,* ISTVAN SCHISZLER,* YUTAKA TOMITA,† MIYUKI UNEKAWA,* HARUKI TORIUMI,* NORIO TANAHASHI,‡ AND NORIHIRO SUZUKI*

*Department of Neurology, School of Medicine, Keio University, Tokyo, Japan; †Institute of Brain and Blood Vessels, Department of Neurology, Mihara Memorial Hospital, Isesaki, Gunma, Japan; and ‡Department of Neurology, Saitama Medical University, Moroyamamachi, Irumagun, Saitama, Japan

ABSTRACT

High-speed camera investigation of rapidly moving red blood cells (RBCs) in the microvasculature has been limited by an inability to handle the vast volume of data. We have developed a novel method to analyze large numbers of RBC images captured by a high-resolution, high-speed camera fitted on a confocal fluorescence microscope, to determine the velocities of individual RBCs in capillaries *in vivo*. Fluorescein isothiocyanate (FITC)-labeled RBCs flowing in the microvasculature of the cerebral cortex of urethane-anesthetized Wistar rats were recorded through the skull window on video clips during specified periods at high frame rates (500 fps). Sequential frames of moving RBCs in the video clips for a specified period were analyzed offline with in-house software (KEIO-IS2). Images of RBCs acquired were numbered automatically in order of appearance and displayed in a two-dimensional (2-D) RBC tracking map. The velocities of individual RBCs were automatically computed based on the RBC displacement per frame multiplied by the frame rate (fps), and the results were displayed in a 2-D velocity map and a 2-D RBC number map. Single capillaries were identified by staining with FITC-dextran. The mean capillary velocity of RBCs was evaluated as 2.05 ± 1.59 mm/second in video clips obtained at 500 fps. This method is considered to have wide potential applicability.
Microcirculation (2008) **15**, 163–174. doi:10.1080/10739680701567089

KEY WORDS: RBC velocity distribution, cerebral cortex, cranial window, capillary flow, rat, confocal microscope

Unlike capillaries in the membranous mesentery, those of organs such as the brain are difficult to access. Nevertheless, capillary red blood cell (RBC) flow in the brain is important, since delivery of RBCs, the major carrier of oxygen, is critical for neuronal metabolism and function. Various sophisticated methods have been developed to address this question, including intravital fluorescence videomicroscopy [4], two-photon laser scanning microscopy [2, 6, 7], an optical method [9, 15], confocal laser scanning fluorescence videomicroscopy [11], scanning laser Doppler flowmetry [1], and MASCOT (Measurement and Analysis System for Capillary Oxygen Transport) [5]. However, these manual analyses have difficulty in handling the vast numbers of relevant RBCs with complex time-to-time variability in the brain tissue under physiological and pathological conditions. In addition, the conventional methods at low frame rates miss high-speed RBCs, which appear in one frame, but are missing in the next frame 1/30 second (or 1/60 second if the fields are deinterlaced) later, so that the apparent average RBC velocity, calculated without consideration of these undetected, rapidly moving RBCs, is not accurate. Here, we report on a new automated method, with high resolution in both space and time, for the imaging and mapping of RBC tracking, RBC number, and RBC velocity in a region of interest (ROI) *in situ*. We demonstrate the practical feasibility of the method and describe its validation.

This work was supported by JSPS Grant-in-Aid #17390255. The authors have no conflicts of interest.

Address correspondence to Minoru Tomita, Department of Neurology, School of Medicine, Keio University, 35 Shinanomachi, Shinjuku-ku, Tokyo 160-8582, Japan. E-mail: mtomita@sc.itc.keio.ac.jp

Received 15 February 2007; accepted 11 July 2007.

MATERIALS AND METHODS

Equipment Assembly and Image-Analyzing Software (KEIO-IS2)

The assembly of the high-speed camera laser-scanning confocal fluorescence microscope system comprises an objective lens (LU Plan EPI SLWD 20x N.A. = 0.35, and 50x N.A. = 0.55), or water immersion lens (Plan Fluor 20x W N.A. = 0.50 and Plan Fluor 60x W N.A. = 1.00; Nikon, Tokyo, Japan), an argon laser ($\lambda = 488$, Melles Griot, Carlsbad, CA, USA), a multibeam confocal scanning unit (CSU22; Yokokawa, Tokyo, Japan), an image intensifier (C6653MOD-N; Hamamatsu Photonics, Hamamatsu, Japan), a MotionPro high-speed camera (Model 500; frame rate of 60, 125, 250, and 500 fps, and electronic shutter speed [exposure time] of 1/60, 1/125, 1/250, 1/500, and 1/1000 seconds) with a digital imaging system with the MiDAS program file (RED-Lake, San Diego, CA, USA). A halogen lamp (Model LH-M100CR-1; Hoya Ltd., Tokyo, Japan) installed in the assembly is used for viewing the field and for online continuous videorecording with a video camera (30 fps, DCR-PC100; Sony, Tokyo, Japan). The high-speed system enabled us to acquire images of fluorescein isothiocyanate (FITC)-labeled RBCs flowing in capillaries at 60 (Figure 1A), 125, 250, and 500 fps (Figure 1B). The shutter speed (exposure time) for the acquisition of all images in the present experiment was set at 1/fps; namely, a 1/250 second shutter speed at 250 fps and 1/500 second at 500 fps. The working distance from the objective lens to the brain surface was ca. 1.0 cm (except for the water immersion lens), which was convenient to allow for the placement of electrodes for concomitant measurements of parameters such as the electroencephalogram (EEG), field DC potential, gases and pH, and also permitted the direct application of gases or pharmacological agents to the brain surface.

The image signal through the objective lens was switched either to the high-speed camera system or to the conventional slow-video (30 fps) system [10]. Images acquired with the high-speed system were stored in discrete video clips of up to 6000 frames each (24 seconds at 250 fps and 12 seconds at 500 fps) in an uncompressed AVI file format on hard disk drives of terabytes. A selected video clip was transferred to a PC and analyzed in a MATLAB® (The Math Works, Inc., Natick, MA, USA) environment, using application software (KEIO-IS2) developed by one of the present authors (I.S.) [10]. The program exploits the above-threshold light intensity

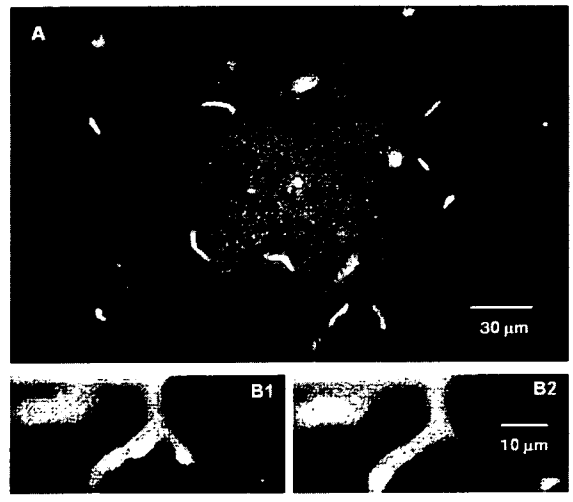

Figure 1. Fluorescein isothiocyanate–labeled red blood cells (RBCs) as viewed with the 60 fps video camera (A) and those at a branching capillary as viewed with the high-speed camera confocal fluorescence microscope system (B1 at control with the 500 fps and B2 at 5/500 second [five frames] later). The manually calculated RBC velocity in the left branch was 1.5 mm/second and that in the right branch was 3.0 mm/second.

of bright, round particles (i.e., FITC-labeled RBCs) on a dark background to track particles automatically. The software is customized by setting several parameters in the dialog box menu of KEIO-IS2, as shown in Figure 2 (right column). First, gray-level thresholding (threshold level = ca. 10–20%) was applied automatically to each frame to differentiate FITC-labeled RBCs from the background, and then all particles having at least eight connected pixels were recognized as RBCs (RBC size threshold = 8). Scale was set at 1 μm/pixel, maximum RBC displacement distance from the original position (Search radius, RBC distance between two frames) at 20 μm, the minimum number of frames of RBC movement (Minimum frames of RBC movement) as three, and the minimal flow velocity (Velocity threshold) as 30 μm/second or 0.03 mm/second. These settings were all selected based on trial and error and confirmed to be appropriate by the method validation. Next, a file (a data set of a video clip) was selected (Select a file), and the number of frames to be analyzed was set by specifying the first frame (First frame) and last frame (Last frame) of the video clip. The computer then conducted the calculations automatically when the RBC tracking button was clicked. Conditions of frame analysis for a data set of a video clip are described in square brackets (with or without

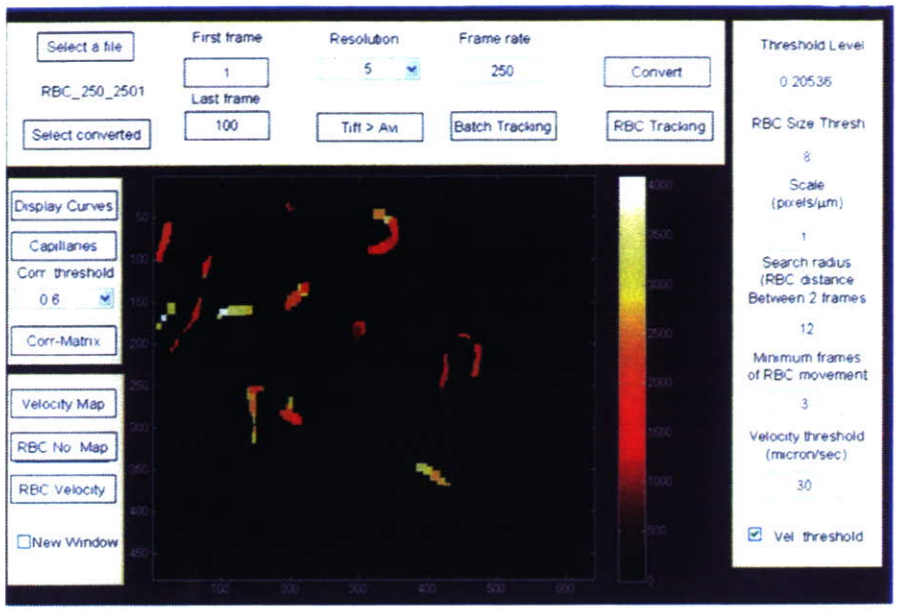

Figure 2. Dialogue box menu of KEIO-IS2. See the text for an explanation. When red blood cell "(RBC) tracking" is clicked, the computer automatically yields the RBC tracking map (T map), RBC velocity map (V map), RBC number map (N map), and a list of numerical velocities of all mean RBCs appearing in the region of interest of 450 × 500 μm. In the figure, the V map is displayed. Color changes indicate velocity changes (scaled in the right bar).

a data subset identification, i.e., the experiment number, as a postfix) as follows: number of frames used for the analysis with the first frame to the last frame as subscripts, and frame rate at image acquisition. For example, the data subset $[1000_{1\text{-}1000}, 250]_{20\text{-}1}$ means 1000 frames from the first frame to the 1000th frame clipped from data set 1 of experiment no. 20–1 acquired at 250 fps. In this paper, the same data subset $[1000_{x1\text{-}x2}, 250]_{20\text{-}1}$ was used throughout for the analyses shown in Figures 2, 3, 5, 6, 7, 8, and 9 to maintain consistency. When the RBC tracking button is clicked, the computer starts to search for FITC-labeled RBCs in the ROI frame by frame, calculating the centroids of the recognized RBCs at the geometric center of the connected pixels, and positioning them in the matrix automatically. The displacements of the centroids detected in subsequent frames were measured, and the velocities of individual RBCs in mm/second were immediately calculated from the respective displacement distances of the centroids divided by the frame interval. The computer continued the calculations, automatically numbering RBCs in the order of appearance, frame by frame for consecutive frames from the specified first frame to the specified last frame. The time required for the calculation of the 1000 frames (4 seconds for the acquisition) was ca. 5 minutes with our computer (Sony VAIO, PCV 1140; Tokyo, Japan). After the calculation had been done for the 1000 frames (4 seconds) in the data subset, the computer yielded three maps: an RBC tracking map (T map) in which automatically numbered RBC tracks are shown in different colors, an RBC velocity map (V map) with a color scale, and an RBC number map (N map) obtained for the 4-second interval in this case. However, the interval has to be standardized to per unit time for comparison of N maps in different groups. Parts of the RBC tracking map can be enlarged to see the details of RBC movements in a new window (New window), and the interrelationship between individual RBCs that passed through the same single capillaries can be seen by selecting a small area on the T map. The velocity data with identification numbers were then exported to a spreadsheet (Microsoft® Excel, Redmond, WA, USA) where the average velocities of all detected individual RBCs that appeared in the ROI during the specified period were listed, and were subjected to classification into various categories for statistical treatment. Capillary data in this data subset were sorted in the order of appearance and diagrammed (Velocity diagram), or in the order of magnitude for presentation as a histogram, which illustrated the RBC velocity profile in the ROI during the specified period (Velocity profile). Employing this analytical

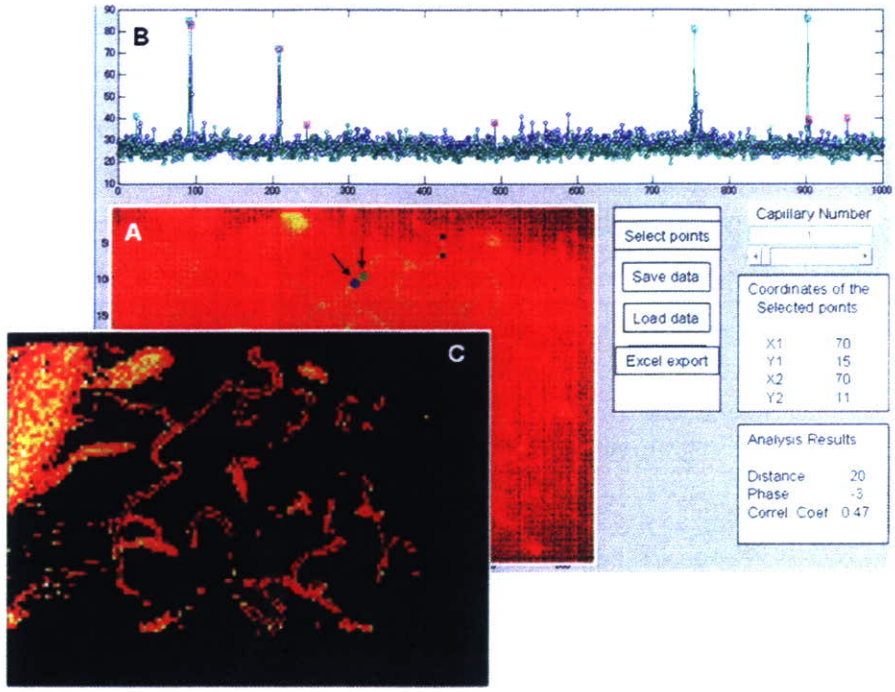

Figure 3. (**A**) A capillary image obtained by the analysis of 1000 frames (see text). At the two arrows, sequential red blood cell (RBC) pulse train records were generated, as shown in (**B**). (**C**) is the built-up image based on correlation coefficients (above 0.4) of RBC tracing curves between neighboring pixels in matrices. This image exhibits the microvascular architecture in the cerebral cortex sliced at a level of 50 μm in depth with the confocal microscope.

technique, we calculated single-capillary velocities in 37 rats and obtained 4252 RBC velocities from approximately 100 samples each. The results were displayed as a frequency distribution function of capillary velocity [16]. In calculating the RBC velocities, the software made no correction for movement along the z-axis, but simply expressed the results as a two-dimensional (2-D) (x-y) RBC velocity map.

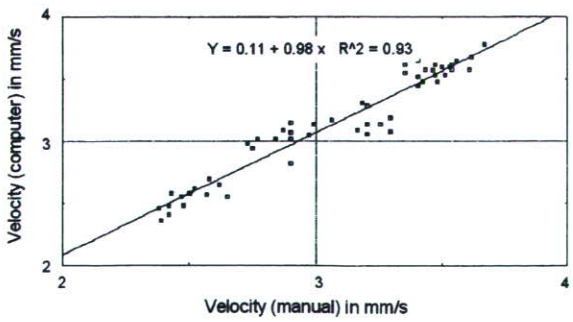

Figure 4. There is a linear correlation between red blood cell velocity manually calculated (x) and that automatically calculated with KEIO-IS2 (y).

The software KEIO-IS2 has an additional function to visualize the microvascular architecture in the tissue. The data subset $[1000_{1\text{-}1000}, 250]_{20\text{-}1}$ consists of 1000 sequential frames recording changes in focal brightness reflecting the passage of FITC-labeled RBCs. If we simply stack all these frames to produce a single picture, we obtain an image of the vessels, as shown in Figure 3A, since bright FITC-labeled RBCs are present only in vessels. However, this image is not sufficiently clear. KEIO-IS2, therefore, employs the following method to visualize the microvascular architecture. When the changes in brightness are recorded at the two pixels shown by green and blue (arrows) on the capillary image in Figure 3A, the two records of pulse trains shown in green and blue were obtained (Figure 3B). The computer immediately calculated the distance between the two pixels, the phase delay, and the correlation coefficient of the two pulse train records. The correlation coefficient between neighboring contiguous pixels on the same capillary is naturally high. The computer calculates all correlation coefficients between pixels in matrices and shows them in specified colors according to their magnitude. By displaying pixels with correlation

Figure 5. The similarity between the microvascular architecture computationally visualized using KEIO-IS2 (**A**, **B**) and that seen in a microtomed Mercox cast of rat brain microvasculature (**C**).

coefficients above a certain threshold (e.g., $r > 0.6$), an image of the microvascular architecture is built up, as shown in Figure 3C.

Validation of the Method

A thin, straight glass capillary tube (ca. 20 μm intradermally) was used to validate the calculated velocities of FITC-labeled RBCs made to flow at various rates with an infusion pump. Flowing RBCs were videotaped at 60 fps, and the velocities of individual RBCs were first manually calculated in a frame-by-frame fashion, with the RBCs numbered in the order of appearance. The results were then compared with these values generated automatically with the computer, correlating RBCs in the same order of appearance (Figure 4). Next, to confirm that what we are looking at is actually the intraparenchymal capillary network, we compared the microvascular architectures obtained by two entirely different methods: one was the architecture computationally constructed with KEIO-IS2 at the intraparenchymal level of the *in vivo* cerebrocortical microvasculature (see above), and the other was the angioarchitecture produced from a microtomed (10-μm slices) Mercox cast of rat cortical vasculature. A liquid acrylic resin (Mercox, Resin, Ladd Research, Williston, VT, USA) was injected into the heart to fill the cerebral microvasclature via the carotid artery in a rat, then the head was guillotined and soaked in a strong acid for 3 weeks. The microvascular moulded cast was taken out, washed, and embedded in polystyrene. After hardening of the plastic spacer, the cast was microtomed into 10-μm slices. The cut surface of the intraparenchymal microvasculature thus visualized was viewed with a microscope and photographed.

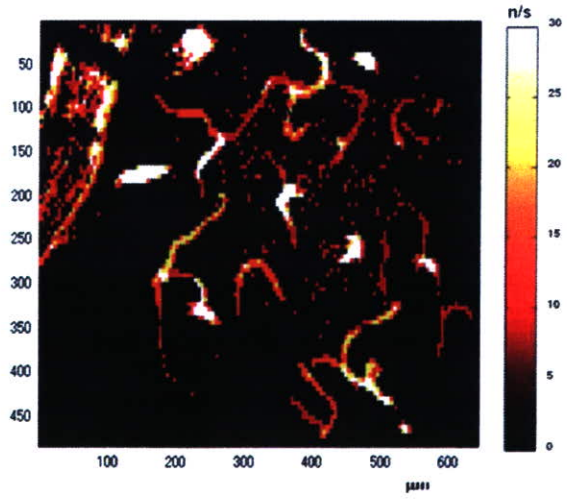

Figure 6. Red blood cell (RBC) number map (N map, which represents all RBCs that appeared in the region of interest during 4 seconds, or integration of all 1000 frames) calculated from a data subset $[1000_{1\text{-}1000}, 250]_{20\text{-}1}$. Note that the N map resembles the microvascular structure based on correlation coefficients (see Figures 3C and 5A).

Animal Preparation and Experimental Protocol

Wistar rats of both sexes were used with the approval of the Animal Ethics Committee of Keio University (Tokyo, Japan), and all experimental procedures were in accordance with the university's guidelines for the care and use of laboratory animals. Each rat, under anesthesia induced with halothane followed by intraperitoneal 10% urethane (1 mL/100 g body weight), was fixed to a head holder, and a window of approximately 4 mm was opened in the skull at the parietotemporal region of the cerebral cortex. Subsequent surgical operations were carried out under a Carl Zeiss Surgical Microscope (Carl Zeiss, GmbH, Oberkochen, Germany) The dura was removed and the exposed cortex was covered with a quartz cover

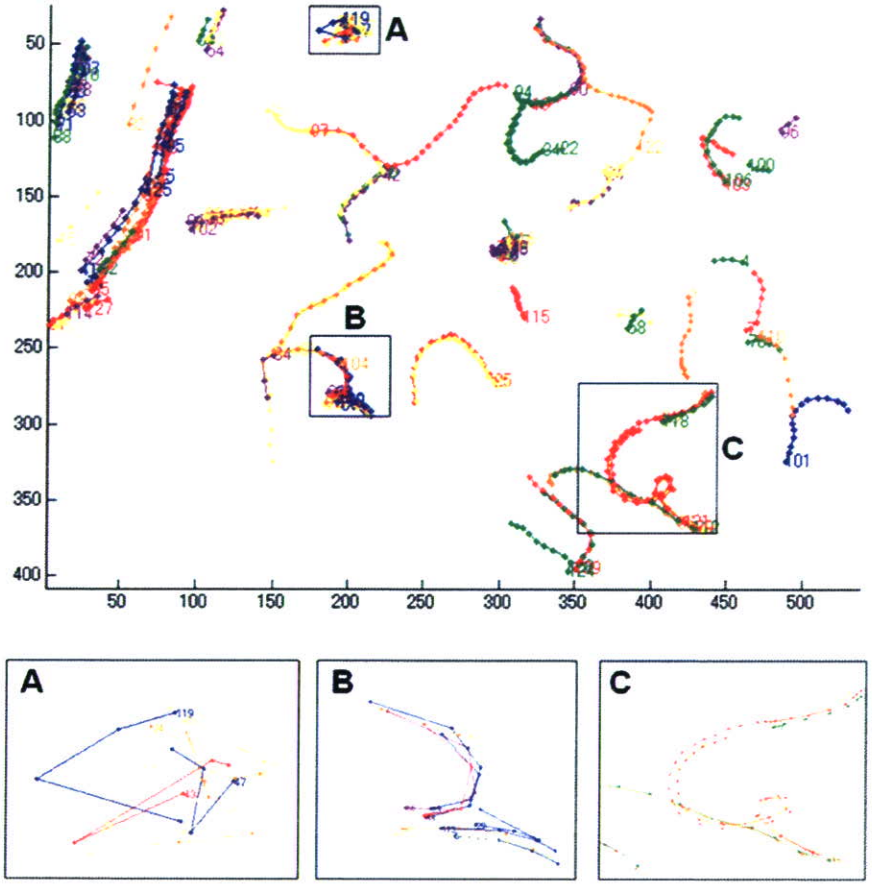

Figure 7. Red blood cell (RBC) tracking map obtained after analysis of the data subset $[1000_{1\text{-}1000}, 250]_{20\text{-}1}$. Frame-by-frame movements of all RBCs are shown. RBCs were automatically numbered in order of appearance. The bottom three figures are enlargements of capillary RBC tracking at **A**, **B**, and **C**.

slip. The rat was placed on the stage of a microscope having x-y-z knobs with a head holder, which fixed the head with ear bars, so that the center of the skull window was positioned under the objective lens of the microscope. A femoral artery and a femoral vein were catheterized for systemic arterial blood pressure (SABP) monitoring and the injection of the FITC-labeled RBC suspension, respectively.

After the selection of an appropriate capillary-rich ROI at around 50 μm in depth in the cerebral cortex, the routine experimental procedure was as follows: (i) We started color video (30 fps) recording of the intraparenchymal microvasculature under cold light (PL075; Hoya Scott, Tokyo, Japan), and recording was continuous throughout the course of the experiment; (ii) the FITC-labeled RBC suspension (0.5 mL) was injected into the circulating blood via the femoral vein. The bright RBCs appeared like fireflies on a dark background in the ROI (Figure 1A) and remained circulating for more than 3 hours at a concentration of ca. 0.4% of total RBCs. Prerequisite assumptions are that FITC-labeled RBCs *in situ* behave in the same manner as the unlabeled majority of RBCs, and that the mixing was complete, so that the labeled RBCs were representative of circulating RBCs; (iii) the slow video system was switched to the high-speed system for the recording of RBC movements at 60–500 fps under confocal laser beam (488 nm) illumination. The exposure time of the brain to the laser beam was usually less than 5 minutes in total, to avoid irradiation damage to the tissue; and (iv) an aliquot of 0.2 mL of 0.25% FITC-dextran (70 kD) was injected into the femoral vein at the end of the experiments to confirm capillaries and to allow for a retrospective merging of the capillary images with RBC tracking maps. Initially, this procedure

No	V (mm/s)
1	2.8308
2	0.9781
3	1.8019
4	1.6386
5	1.7615
6	3.5649
7	1.5369
8	1.1970
9	2.5069
10	1.5478
11	2.5305
12	0.8186
13	1.863
14	1.6163
15	3.3802
=	=
115	0.3781
116	0.4519
117	0.4612
118	1.4936
119	2.9507
120	0.7378
121	1.9141
122	1.7185
123	1.8065
124	1.4869
125	2.6957
126	0.7652
127	1.3077

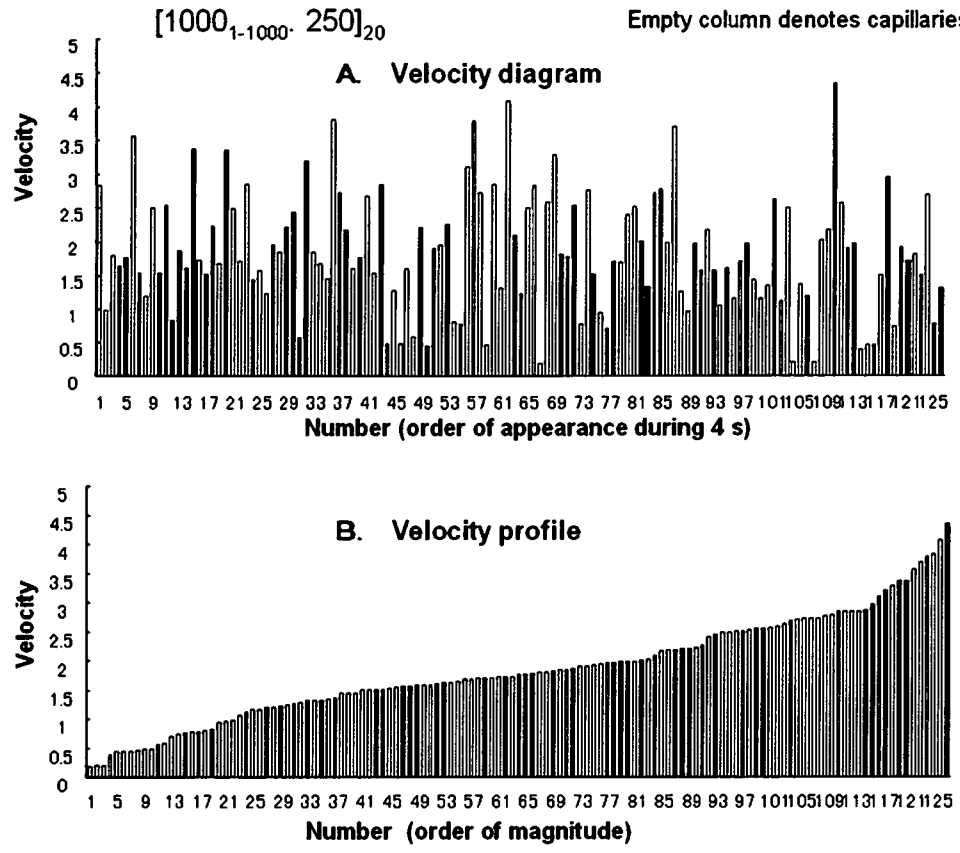

Figure 8. Left: Part of an Excel spreadsheet listing individual mean values of red blood cell (RBC) velocities with their identification numbers in order of appearance (capillary RBCs are underlined). (**A**) Diagramatic presentation of the mean RBC velocities. The x-axis is the order of appearance. (**B**) Velocity diagram in order of magnitude. It should be noted that RBC velocities in capillaries (closed bars) are not clustered, but are rather widely dispersed.

was carried out at the beginning of the experiments because it was easy to identify capillaries and to measure capillary diametric changes. We defined FITC-dextran-stained vessels having $<10\ \mu$m diameter and showing RBC passage as capillaries. However, we noticed that the amount of FITC-dextran required to clearly visualize the capillary wall not only increased the background brightness, which sometimes disturbed the detection of FITC-labeled RBCs, but also caused microvascular derangement. Therefore, the confirmation of capillaries by this technique was made at the end of the experiments only in 20 cases; in all these cases, the stained capillaries corresponded with high fidelity to the capillaries separated by cluster analysis based on the criterion of single-file tracking of RBCs, so that in the remaining cases, only a cluster analysis was used.

In general, the number of frames generated by the high-speed camera was large (of the order of 15–20 GB), so the files were stored in external hard disks with terabyte capacity, usually as 10–20 separate data sets of video clips in AVI files of 6000 frames (12 seconds at 500 fps; 24 seconds at 250 fps) each in an experiment. Further division of video clips into data subsets of smaller numbers of frames, mostly 100, 500, or 1000 frames, was done for offline analysis with KEIO-IS2 to measure RBC velocities.

In all experiments, SABP (systemic arterial blood pressure) was routinely recorded, via a strain gage transducer connected to the femoral arterial catheter, on a PC with Acqknowledge software (MP 100 WS, BIOPACK Systems, Inc., Goleta, CA, USA). Arterial blood was withdrawn from the femoral artery, and arterial gases and pH were measured in 4 cases before and after the experiments, employing a gas pH meter (Chiron Diagnostics 248, Medfield, MA, USA). When required, tissue blood flow was measured by a bolus injection of saline via a catheter inserted into

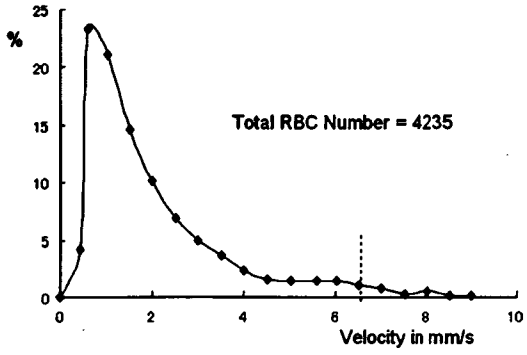

Figure 9. Frequency distribution function of red blood cell (RBC) velocities. RBC velocities higher than 6.5 mm/second could be excluded from capillary group with statistical significance, even though the vessel size was the same as that of the capillaries (see text for explanation).

the external carotid artery and retrogradely advanced to the bifurcation, so that the saline produces cortical tissue hemodilution curves through the internal carotid artery. The technique has been reported elsewhere [9]. The reciprocal mean transit times [14] were calculated in all matrices and exhibited as a 2-D flow map, with automatic calculation of the mean and standard deviation with the KEIO-IS1 software [14]. The conversion of units from mean transit time [seconds^{-1}] to flow [mL.g^{-1}. minutes^{-1}] was done by using a factor of 60 × 0.05 on the assumptions that water-specific gravity [g.mL^{-1}] = 1 and CBV (cerebral blood volume) = 5%.

RESULTS

General Observations

The experiments were performed on more than 100 rats, though 5 rats were unsuccessful because of bleeding either in the cerebral cortex or from an artery during catheter mishandling. We obtained more than 1000 data sets (average, 10 data sets of 6000 frames from each experiment). Usually, we analyzed subsets of 100–1000 frames clipped from a data set with KEIO-IS2. The reproducibility of the analysis with KEIO-IS2 on the same video clip was excellent. Even inexperienced experimenters obtained exactly the same T map, N map, and V map with precisely calculated RBC velocities as highly experienced investigators, simply by running KEIO-IS2 for any data set with specification of the first and last frames (Figure 2).

The physical condition of the rats in the successful experiments remained broadly unchanged for approximately 3 hours during the experiments, during which time FITC-labeled RBCs were present in the circulating blood, and the cerebral cortex was exposed to the laser beam (488 nm) for discrete periods, totaling approximately 5 minutes. The values of physiological parameters before and after experiments were as follows: SABP changed from 110 ± 8.5 to 108 ± 13.2 mmHg ($n = 52$); arterial PO_2 changed from 105.6 ± 5.1 to 101.1 ± 6.50 mmHg, arterial PCO_2 changed from 51.2 ± 2.6 to 53.9 ± 4.7 mmHg, and arterial pH changed from 7.38 ± 0.04 to 7.34 ± 0.03 ($n = 4$); average tissue blood flow measured by a hemodilution technique [9, 13, 14, 15] changed from 6.42 ± 0.48 to 5.94 ± 2.64 mL.g^{-1}.minutes^{-1} ($n = 13$). None of the differences of these parameter values before and after experiments are statistically significant.

Validation of the Method In the *in vitro* test employing a glass tube, we observed a good linear correlation between the velocities manually calculated (x) and those calculated with the computer (y), yielding the regression line $y = 0.98x + 0.11$. The correlation was statistically significant ($r^2 = 0.93$, $P < 0.001$). The numbers of FITC-labeled RBCs measured directly and evaluated by the computer corresponded well, supporting the validity of the computer method. In *in vivo* experiments where FITC-labeled RBCs were moving three-dimensionally (3-D) in the microvasculature, as shown in Figure 2A, we observed an elongation of RBCs at 60 fps. We found that the magnitude of elongation of the RBC (y) was broadly linearly related to the velocity (x) (regression line $y = 0.91x + 3.4 + L$ [$r^2 = 0.74$, $P < 0.01$] at 60 fps), where L is the diameter of the stationary RBC (i.e., 7.5 μm). However, as shown in Figure 1B1 and 1B2, images of RBCs in capillaries acquired at 500 fps exhibited an oval shape, showing minimal elongation (see Discussion). The equation for RBC elongation no longer holds at a high fps.

Figure 5A is a binary map of Figure 3C, and Figure 5B is the trace of the contour of the vessels. The resulting image (Figure 5B) is quite similar to Figure 5C, which shows the microvascular bed as visualized in a microtomed section of a microvascular moulded cast (Mercox) hardened in polystyrene. The similarity implies that (i) what was recognized by the computer originated from FITC-labeled RBCs filling the vasculature, (ii) the computer faithfully reconstructed the angioarchitecture of the cortical microvascular network in the cerebral cortex, and (iii) the depth of focus of the lens covered a thin

vascular layer with the thickness of at least 10 μm at a depth between 0 and 100 μm from the pia mater.

RBC Tracking in All Vessels in the ROI Analysis with KEIO-IS2 of a data subset $[1000_{1\text{-}1000}, 250]_{20\text{-}1}$ yielded the illustrated V map (Figure 2), N map (Figure 6), T map (Figure 7), velocity diagram (Figure 8A), and velocity profile (Figure 8B). The N map, which consists of integrated images of the RBC number at each pixel, resembled the correlation map shown in Figures 3C and 5A. The T map (Figure 7) exhibits all labeled RBCs appearing in the ROI over a period of 4 seconds (1000 frames in total). The files of RBC tracking were numbered automatically in order of appearance in different colors. Since most of the RBCs exhibited single-file tracking, they were considered to represent mostly capillaries. Detailed tracing of RBCs in single capillaries was done using an enlargement technique, as shown in Figure 7A, 7B, and 7C. However, an automated calculation did not allow us to distinguish RBCs in capillaries from those in arterioles and venules. When capillaries had been stained with FITC-dextran beforehand, capillaries could be identified very easily, but we found that FITC-dextran damaged endothelial cells. For this reason, capillary staining was done in only 20 cases at the end of experiments. The procedure of capillary staining was omitted in the majority of cases, because the results of capillary identification using this method coincided so well with putative capillaries identified simply on the criterion of single-file RBC tracking in the T map. Separation of capillary RBCs was thus done simply by cluster analysis based on a criterion of single-file RBCs in the tracking map.

All the computed RBC velocity data with their identification numbers in the subset ($[1000_{1\text{-}1000}, 250]_{20\text{-}1}$) were exported to a spreadsheet (Microsoft® Excel), which contained 128 RBCs in total and 39 capillaries (underlined in the table in Figure 8) that appeared in the ROI during the 4 seconds in this particular case. Figure 8A shows the velocity diagram, in which 128 mean individual RBC velocities are illustrated in order of appearance. The closed columns indicate RBC velocities in capillaries identified by staining with FITC-dextran in this case. When the capillary data were sorted by order of magnitude of the velocity, we obtained the velocity profile shown in Figure 8B. It should be noted that RBC velocities in capillaries do not cluster in a certain velocity range, but are rather dispersed, making it difficult to discriminate capillaries just from the magnitude of the RBC velocity.

In general, we found that the mean magnitudes of RBC velocity were different in all cases, depending on how many arterioles and/or venules were included in the ROI. Even in a single experiment, mean RBC velocity values of all vessels varied dynamically, with apparent oscillations.

RBCs in Single Capillaries

Analysis of RBCs exclusively in single capillaries in a ROI afforded mean capillary RBC velocity values (mean ± SD). However, we found that the mean velocity differed, depending upon the frame rate: 0.72 ± 0.51 mm/second at 60 fps ($n = 3$), 0.93 ± 0.86 mm/second at 125 fps ($n = 11$), 1.46 ± 0.77 mm/second at 250 fps ($n = 15$), and 2.33 ± 1.96 mm/second at 500 fps ($n = 15$). All pairs of mean velocity values at different frame rates were found to be statistically significantly different ($P < 0.05$; Student's t-test, nonparametric). The difference was due to higher speed RBCs, which were missed (i.e., uncounted) at lower frame rates. When the mean velocity was plotted against the frame rate, the regression line showed a correlation coefficient r^2 of 0.998 ($P < 0.001$). We suggest that the real average RBC velocity in single capillaries would be greater than 2.33 mm/second if a much faster camera were used. Occasionally, we fortuitously observed extraordinarily high-speed movement of RBCs (e.g., 9.5 mm/second) in single capillaries. Figure 9 shows the frequency distribution function of 4252 RBC velocities at 500 fps in capillaries selected from 37 rats. The velocity ranged from 0.15 to 9.40 mm/second with a mean of 2.05 ± 1.59 mm/second. Although the RBC velocity increase appeared continuous, we statistically tested the RBC velocity value (X) under the hump based on $(\bar{x} - X)/s$, where $\bar{x}$ is the mean, and s the standard deviation [3]. We found that the capillaries having a RBC velocity higher than 6.5 mm/second were statistically significantly excluded ($P < 0.01$). Thus, the vessels that allowed a fast transit of RBCs seem to belong to a noncapillary group, even though their diameter is the same as that of the capillaries. Figure 10A shows the spatiotemporal heterogeneity of capillary RBC flow sampled at 0.4-second intervals. The V maps were calculated from ten sequential data subsets: $[100_{1\text{-}100}, 250]_{20\text{-}1}$, $[100_{101\text{-}200}, 250]_{20\text{-}1}, \ldots [100_{901\text{-}1000}, 250]_{20\text{-}1}$. The average RBC velocities/numbers exhibit fluctuation, as shown in Figure 10B (left) and the corresponding N maps (Figure 10B, right). Basically, there were no

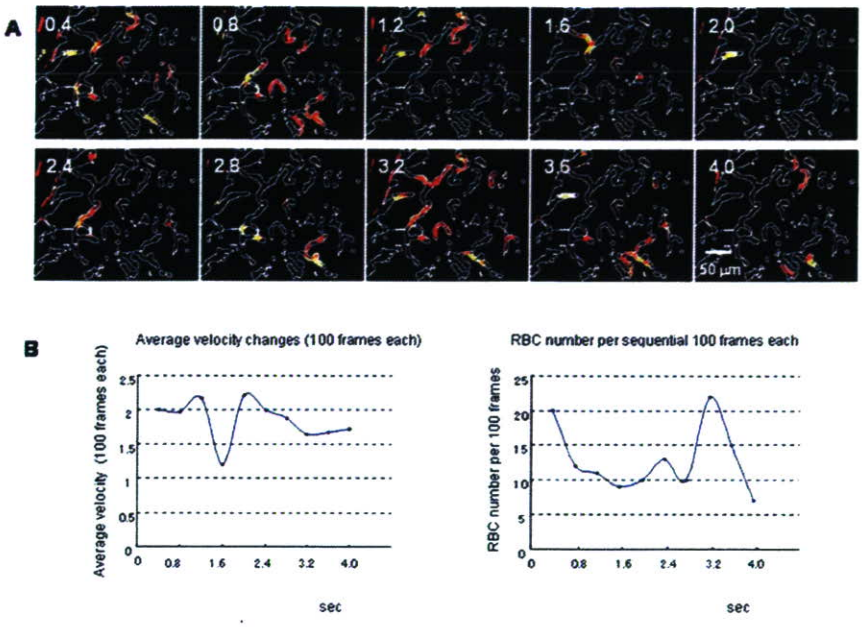

Figure 10. (**A**) A panoramic presentation of red blood cell (RBC) flow heterogeneity in space with time. The numeral at the shoulder of each image is the time after the start in seconds. Note the time-to-time variability in spatial orientation of RBCs. (**B**) Fluctuations in average RBC velocity and in RBC number.

stationary RBC flows in capillaries when images obtained at a sufficiently high speed were analyzed.

DISCUSSION

We have described an automated method for the high-speed acquisition of small moving targets that makes it possible to handle the vast numbers of FITC-labeled RBCs appearing in a small area of the rat cerebral cortex. We have validated the method and applied it to more than 100 rats for evaluating RBC velocities in single capillaries. We believe it has wide potential applicability to track the movements of RBCs not only in the brain, but also other organs, and not only RBCs, but also other blood cells or blood corpuscles, such as white blood cells, platelets, tumor cells, etc., if they are appropriately fluorescently labeled. One unexpected feature of the results was that the mean apparent RBC velocity increased the frame rate dependently, and the increase was highly statistically significant. This was clearly a methodological artifact, since the actual RBC velocities in the ROI should not have changed with different acquisition speed.

When the camera optically sliced the cerebral capillary network at a thickness of ca. 20 μm, the slice would contain numerous short, tortuous capillaries (see Figure 5). Rapidly moving RBCs in these short capillaries disappeared before the computer could capture them in the subsequent frame when a low frame rate was used [16]. These rapidly moving RBCs would, therefore, be missed and uncounted, so that the calculated average RBC velocity at a lower frame rate would be lower. Because higher velocity RBCs can be detected when analyzing images obtained at 500 fps, it is not surprising that the average RBC velocity in single capillaries became as high as 2.05 ± 1.59 mm/second. This value is much faster than values reported in the literature (0.5–1.8 mm/second [4]; 1.5 mm/second (8); 0.83 ± 0.46 mm/second during CO_2 exposure [17]), although these reported values are in good agreement with our data measured at 60 fps (0.72 ± 0.51 mm/second). If we could have further increased the frame rate, putatively missing high-velocity (above 10 mm/second) RBCs would have become detectable, and the calculated mean RBC velocity would have taken a much higher value. Recently, preliminary experiments have been done at 1000, 2000, 3000, 4000, and 5000 fps (courtesy of Professor Norio Tanahashi at Saitama Medical School: unpublished data), and as expected, the results revealed that average RBC velocity showed a further increase, with the fastest moving RBCs having a velocity of 15 mm/second or more. The capillaries

involved had the same diameter as other capillaries in which RBCs were moving at velocities close to the mean. As noted above, statistical analysis indicated that such capillaries with extraordinarily high RBC velocities seem to belong to a separate category from usual capillaries. They may represent thoroughfare channels or preferential channels, but further study is needed on this issue. When we recalculated the mean RBC velocity after the exclusion of RBCs traveling faster than 6.5 mm/second, a value of 1.89 ± 1.32 mm/second was obtained.

The question of the discrepancy between velocities calculated based on successive positions of the centroid or the leading edge of greatly elongated RBCs deserves specific comment. The RBCs appear elongated (Figure 1A) in images acquired at 60 fps, and when these images are used in our automated computer system for velocity estimation, certain errors arise when the degree of elongation of a RBC in the images changes, as will occur when the RBC speeds up or slows down (e.g., at the junctions of capillaries). This error is greatly lessened by the use of the high-speed camera with an acquisition time (exposure time) of 1/250–1/500 second (at 250–500 fps) as employed in this work. We confirmed that even RBCs moving at 5 mm/second in capillaries appear as oval shapes in images obtained with this high-speed system, so that the difference between the velocities calculated from the leading edge and the centroid would be very small. However, use of the centroid might again become problematic in the case of RBCs traveling at much higher velocities, as might occur in a thoroughfare channel. In this paper, we calculated RBC velocities from images obtained at 60, 125, 250, and 500 fps to examine the frame-rate dependency of calculated velocity, but all measurements were made at a stationary state of flow, so we consider that errors arising from the use of the centroid are negligible here.

CONCLUSIONS

In this paper, the results are limited to data from 100 rats. However, we have found this method to have wide applicability to other animals, including mice, and wide versatility to track movements of other fluorescently labeled cells, such as white cells and platelets.

ACKNOWLEDGMENTS

The present address of Dr. Istvan Schiszler is Petofi utca 4, Torokbalint 2045, Hungary. We thank Professors Jacque Seylaz and Elizabeth Pinard for training Dr. Yutaka Tomita in small animal experimental techniques. We also thank Dr. Hidetaka Takeda, Saitama Hospital, Otsuka Pharmaceutical Co., Ltd., and Mr. Harukuni Tsumura, Sankei, Co., Ltd., for their various assistance and valuable suggestions.

The KEIO-IS1 and KEIO-IS2 programs are freely available to researchers in nonprofit organizations; for details, please contact Minoru Tomita at mtomita@sc.itc.keio.ac.jp.

REFERENCES

1. Akgoren N, Lauritzen M. (1999). Functional recruitment of red blood cells to rat brain microcirculation accompanying increased neuronal activity in cerebellar cortex. *Neuroreport* 10:3257–3263.
2. Chaigneau E, Oheim M, Audinat E, Charpak S. (2003). Two-photon imaging of capillary blood flow in olfactory bulb glomeruli. *Proc Natl Acad Sci USA* 100: 13081–13086.
3. Grubbs FE. (1950). Testing outlying observations. *Ann Math Stat* 21:27–58.
4. Hudetz AG. (1997). Blood flow in the cerebral capillary network: a review emphasizing observations with intravital microscopy. *Microcirculation* 4: 233–252.
5. Japee SA, Pittman RN, Ellis CG. (2005). Automated method for tracking individual red blood cells within capillaries to compute velocity and oxygen saturation. *Microcirculation* 12:507–515.
6. Kleinfeld D. (2002). Cerebral blood flow through individual capillaries in rat vibrissa S1 cortex: stimulus-induced changes in flow are comparable to the underlying fluctuations in flow. In: Tomita M, Kanno K, Hamel E (Eds.), Brain Activation and CBF Control. Elsevier Science, BV, ICS 1235, Amsterdam, pp 115–122.
7. Kleinfeld D, Mitra PP, Helmchen F, Denk W. (1998). Fluctuations and stimulus-induced changes in blood flow observed in individual capillaries in layers 2 through 4 of rat neocortex. *Proc Natl Acad Sci USA* 95:15741–15746.
8. Pawlik G, Rackl A, Bing RJ. (1981). Quantitative capillary topography and blood flow in the cerebral cortex of cats: an *in vivo* microscopic study. *Brain Res* 9:208, 35–58.
9. Schiszler I, Tomita M, Fukuuchi Y, Tanahashi N, Inoue K. (2000). New optical method for analyzing cortical blood flow heterogeneity in small animals: validation of the method. *Am J Physiol* 279:H1291–H1298.
10. Schiszler I, Takeda H, Tomita M, Tomita Y, Osada T, Unekawa M, Tanahashi N, Suzuki N. (2005). Software (KEIO-IS2) for automatically tracking red blood cells (RBCs) with calculation of individual RBC velocities

in single capillaries of rat brain (abstract). *J Cereb Blood Flow Metab* 25(Suppl. 1):S541.

11. Seylaz J, Charbonne R, Nanri K, Von Euw D, Borredon J, Kacem K, Meric P, Pinard E. (1999). Dynamic *in vivo* measurement of erythrocyte velocity and flow in capillaries and of microvessel diameter in the rat brain by confocal laser microscopy. *J Cereb Blood Flow Metab* 19:863–870.
12. Tomita M. (1988). Significance of cerebral blood volume. In: Tomita M, Sawada T, Naritomi H, Heiss WD (Eds.), Cerebral Hyperemia and Ischemia—From the Standpoint of Cerebral Blood Volume. Excerpt Med, ICS 764, Elsevier, Amsterdam, pp. 3–31.
13. Tomita M, Gotoh F, Sato T, Amano T, Tanahashi N, Tanaka K, Yamamoto M. (1978). Photoelectric method for estimating hemodynamic changes in regional cerebral tissue. *Am J Physiol* 235:H56–H63.
14. Tomita M, Gotoh F, Amano T, Tanahashi N, Kobari M, Shinohara T, Mihara B. (1983). Transfer function through regional cerebral cortex evaluated by a photoelectric method. *Am J Physiol* 245:H385–H398.
15. Tomita M, Schiszler I, Tomita Y, Tanahashi N, Takeda H, Osada T, Suzuki N. (2005). Initial oligemia with capillary flow stop followed by hyperemia during K^+-induced cortical spreading depression in rats. *J Cereb Blood Flow Metab* 25:742–747.
16. Unekawa M, Tomita M, Tomita Y, Osada T, Toriumi H, Suzuki N. (2007). Extraordinary high flow capillaries in the cerebral microvascular network (abstract). *J Cereb Blood Flow Metab* 27(Suppl.): in press.
17. Villringer A, Them A, Lindauer U, Einhaupl K, Dirnagl U. (1994). Capillary perfusion of the rat brain cortex. An *in vivo* confocal microscopy study. *Circ Res* 75:55–62.

日経バイオテク Biotechnology Japan

2007年06月15日

日本血液代替物学会、早大、血液由来のヘモグロビンを使わない次世代人工酸素運搬体を提案

2007年6月14日、慶応大学で日本血液代替物学会年次大会が開催され、人工血液研究の最前線と題するシンポジウムの中で、早稲田大学理工学術院の小松晃之准教授は、アルブミンにヘムを結合させたアルブミン-ヘムについて報告した。

ヘムは2価の鉄を中心に持つポルフィリン化合物。ヘモグロビンは4つのヘムを持つ分子量6万4000のたんぱく質だ。現在、オキシジェニックス（東京・港、大村孝男社長）やテルモが人工酸素運搬体を開発しているが（関連記事1、関連記事2）、これらは日本赤十字社から提供された期限切れの赤血球製剤から精製したヘモグロビンをリポソームに封入して作ったもの。血液型に関係なく利用でき、長期間保存できるなどの利点があるが、ヘモグロビンの安定性の問題や、赤血球製剤からヘモグロビンを精製する過程で病原体が混入する可能性がゼロにはならない、などの課題がある。

一方、アルブミンについては、三菱ウェルファーマや化学及血清療法研究所が遺伝子組み換え技術で製造されたものを医薬品として開発しており、血液由来ではないものがもうすぐ実用化されようとしている。

小松准教授らはアルブミンが脂肪酸と結合することに着目し、アルブミンと結合するヘムを30種類程度化学合成した。ヘムによって酸素親和性が高いものから低いものまでさまざまあり、「用途に応じて使い分けられる」と小松准教授は説明した。ヘムを解離しにくいようにアルブミン-ヘムの表面をPEGで修飾したものを作成し、貧血状態にしたラットに投与した結果、赤血球を投与したのと同様の効果が得られた。これらのことから、血液由来の成分を全く使わない完全合成のアルブミン-ヘムを次世代の人工酸素運搬体として利用できる可能性を示した。さらに小松准教授は、アルブミンのアミノ酸を遺伝子組換えにより3つだけ改変すれば、天然のヘムでも結合し酸素を運搬できるようになることを明らかにした。

小松准教授は、「アルブミン-ヘムは、たんぱく質製剤として利用されているアルブミンを酸素の運搬に使おうというもので、ヘモグロビンを封入したリポソームとはコンセプトが違う。また、リポソームの直径は200nmから250nmだが、アルブミンは8nm程度なので、脳梗塞などの虚血部位への酸素供給など、用途も広がる」と語った。ちなみに、小松准教授はアルブミン-ヘムの適応として、出血ショックの蘇生液、救急車内での酸素供給液、虚血部位への酸素供給液のほか、移植用臓器の灌流液、体外循環回路の補填液などを挙げている。また、天然のヘムを利用しても、「ヘモグロビンを利用する場合と違って感染因子が入り込む可能性はほとんどない」（小松准教授）とのことだ。（橋本宗明）